tory significance by influencing the DNA binding affinity of the proteins (*24*). How these types of interactions might influence the activities of ITF-1 and ITF-2 remain to be determined. It is relevant to note that ITF-1 appears to function as a transcription factor on its own. It contains distinct elements that dictate both efficient DNA binding and transcription activation. Hence, it is unlikely that a second helix-loop-helix protein is required to specifically supply either of those functions. Furthermore, ITF-1 is active in yeast where it is doubtful that such specialized regulatory proteins exist.

REFERENCES AND NOTES

1. J. Banerji, L. Olson, W. Schaffner, *Cell* **33**, 729 (1983); S. D. Gillies, S. L. Morrison, V. T. Oi, S. Tonegawa, *ibid.*, p. 717; M. S. Neuberger, *EMBO J.* **2**, 1373 (1983); M. L. Atchinson, *Annu. Rev. Cell Biol.* **4**, 127 (1988).
2. A. Ephrussi, G. M. Church, S. Tonegawa, W. Gilbert, *Science* **227**, 134 (1985); G. M. Church, A. Ephrussi, W. Gilbert, S. Tonegawa, *Nature* **313**, 608 (1985).
3. H. Singh, R. Sen, D. Baltimore, P. A. Sharp, *Nature* **319**, 154 (1986); L. M. Staudt *et al.*, *ibid.* **323**, 640 (1986).
4. C. L. Peterson, S. Eaton, K. Calame, *Mol. Cell. Biol.* **8**, 4972 (1988).
5. M. Lenardo, J. W. Pierce, D. Baltimore, *Science* **236**, 1573 (1987).
6. M. Kiledjian, L.-K. Su, T. Kadesch, *Mol. Cell. Biol.* **8**, 145 (1988).
7. B. P. Tsao, X.-F. Wang, C. L. Peterson, K. Calame, *Nucleic Acids Res.* **16**, 3239 (1988); J. Perez-Mutul, M. Macchi, B. Wasylyk, *ibid.*, p. 6085.
8. C. Wasylyk and B. Wasylyk, *EMBO J.* **5**, 553 (1986); T. Kadesch, P. Zervos, D. Ruezinsky, *Nucleic Acids Res.* **14**, 8209 (1986); J. Weinberger, P. S. Jan, P. A. Sharp, *Mol. Cell. Biol.* **8**, 988 (1988).
9. C. Murre, P. Schonleber McCaw, D. Baltimore, *Cell* **56**, 777 (1989).
10. R. Sen and D. Baltimore, *ibid.* **46**, 705 (1986).
11. C. R. Vinson, K. L. LaMarco, P. R. Johnson, W. H. Landschulz, S. L. McKnight, *Genes Dev.* **2**, 801 (1988).
12. P. Henthorn, M. Kiledjian, T. Kadesch, unpublished observations.
13. M. J. Weiss *et al.*, *J. Biol. Chem.* **263**, 12002 (1988).
14. C. M. Gorman, L. F. Moffat, B. H. Howard, *Mol. Cell. Biol.* **2**, 1044 (1982).
15. B. C. Rymond, R. S. Zitomer, D. Schumperli, M. Rosenberg, *Gene* **25**, 249 (1983).
16. L. Guarente and M. Ptashne, *Proc. Natl. Acad. Sci. U.S.A.* **78**, 2199 (1981); L. Guarente and T. Mason, *Cell* **32**, 1279 (1983).
17. J. W. Lillie and M. R. Green, *Nature* **338**, 39 (1989).
18. J. Battey *et al.*, *Cell* **34**, 779 (1983).
19. S. J. Tapscott *et al.*, *Science* **242**, 405 (1988).
20. W. E. Wright, D. A. Sasson, V. K. Lin, *Cell* **56**, 607 (1989).
21. J. D. Mellentin, S. D. Smith, M. L. Cleary, *ibid.* **58**, 77.
22. H. Beckmann, L.-K. Su, T. Kadesch, *Genes Dev.* **4**, in press.
23. M. Caudy *et al.*, *Cell* **55**, 1061 (1988); B. Thisse, C. Stoetzel, C. Gorostiza-Thisse, R. Perrin-Schmitt, *EMBO J.* **7**, 2175 (1988); R. Villares and C. V. Cabrera, *Cell* **50**, 415 (1987).
24. C. Murre *et al.*, *Cell* **58**, 537 (1989).
25. Plasmids were constructed using standard techniques (*30*). The βGE2-2 and βGE2-5 constructs were made by replacing the β-globin gene coding region of pT7βΔ6Sal (*31*) with the E2-2 and E2-5 protein-coding regions, respectively. The pSVE2-2 construct was made by replacing the dihydrofolate reductase cDNA of pSV2Adhfr (*32*) with the β-globin 5′ leader, ATG, and E2-2 coding region from βGE2-2. The pSVE2-5 construct was similarly made from βGE2-5. The bacterial *cat* gene reporter plasmids will be described elsewhere (*33*). CYC:E2-5 and CYC:E2-5R were constructed by replacing the GalK gene of YRpR1 (*15*) with the E2-5 cDNA in both orientations. UAS_c:βgal and ΔUAS_c:βgal are pLG669-Z and pLG670-Z (*16*), respectively. $[E5–E2]_4$:βgal was constructed by replacing the UAS sequences of pLG669–Z with four copies of the μE5 + μE2 oligonucleotide. All plasmids expressing GAL4 fusion proteins were derived from $pGAL_{1–147}$ (*17*).
26. P. Henthorn, P. Zervos, M. Raducha, H. Harris, T. Kadesch, *Proc. Natl. Acad. Sci. U.S.A.* **85**, 6342 (1988).
27. H. Beckmann and T. Kadesch, *Mol. Cell. Biol.* **9**, 4535 (1989).
28. F. L. Graham and A. J. van der Eb, *Virology* **52**, 456 (1973).
29. F. Lee *et al.*, *Nucleic Acids Res.* **12**, 4191 (1984).
30. T. Maniatis, E. F. Fritsch, J. Sambrook, *Molecular Cloning: A Laboratory Manual* (Cold Spring Harbor Laboratory, Cold Spring Harbor, NY, 1982).
31. C. Norman, M. Runswick, R. Pollock, R. Treisman, *Cell* **55**, 989 (1988).
32. S. Subramani, R. C. Mulligan, P. Berg, *Mol. Cell. Biol.* **1**, 854 (1981).
33. D. Ruezinsky, H. Beckmann, P. Henthorn, T. Kadesch, manuscript in preparation.

34. We would like to thank R. McCarrick-Walmsley for excellent technical assistance and D. Ruezinsky for the various reporter plasmids carrying the μE5 + μE2 oligonucleotide. Supported by funds from the Howard Hughes Medical Institute (to T.K.).

2 October 1989; accepted 14 December 1989

Glutamate Induces Calcium Waves in Cultured Astrocytes: Long-Range Glial Signaling

ANN H. CORNELL-BELL, STEVEN M. FINKBEINER, MARK S. COOPER, STEPHEN J SMITH*

The finding that astrocytes possess glutamate-sensitive ion channels hinted at a previously unrecognized signaling role for these cells. Now it is reported that cultured hippocampal astrocytes can respond to glutamate with a prompt and oscillatory elevation of cytoplasmic free calcium, visible through use of the fluorescent calcium indicator fluo-3. Two types of glutamate receptor—one preferring quisqualate and releasing calcium from intracellular stores and the other preferring kainate and promoting surface-membrane calcium influx—appear to be involved. Moreover, glutamate-induced increases in cytoplasmic free calcium frequently propagate as waves within the cytoplasm of individual astrocytes and between adjacent astrocytes in confluent cultures. These propagating waves of calcium suggest that networks of astrocytes may constitute a long-range signaling system within the brain.

ASTROCYTES GUIDE NEURONAL DEvelopment, metabolize ions and neurotransmitters, and regulate central nervous system vasculature (*1*), but until recently, there has been little indication that they play any role in rapid signal transmission (*2, 3*). This situation has begun to change with the finding that astrocytes possess ion channels opened on a millisecond time scale by glutamate, the common excitatory neurotransmitter (*3*). In this report we describe another prompt form of astrocytic response to glutamate and observations suggesting that networks of astrocytes may constitute an extraneuronal pathway for rapid long-distance signaling within the brain.

We first examined intracellular free calcium ($Ca^{2+}{}_i$) responses of cultured hippocampal astrocytes to prolonged applications of glutamate (*4, 5*) (Fig. 1). Virtually all cells responded to 100 μ*M* glutamate with an initial spike-like increase in $Ca^{2+}{}_i$, but later phases of the response to the continued presence of glutamate varied from cell to cell (Fig. 1, A to D). We have classified response types into three categories. (i) In the sustained oscillation response, cells exhibited a prolonged episode of $Ca^{2+}{}_i$ oscillation, lasting from 300 to 1800 s (mean ± SD = 850 ± 300 s; measurements on 24 cells, five experiments). In some cells, the oscillation frequency remained relatively constant (Fig. 1E) (period of 13 ± 2 s; 192 measurements on seven cells, three experiments). In other cells, the oscillation frequency gradually decreased (Fig. 1F) (period of initial cycle of oscillation is 9 ± 2 s, increasing to 23± 5 s after 5 min, 31 measurements). (ii) In the damped-oscillation response, cells exhibited $Ca^{2+}{}_i$ oscillations of decreasing frequency (Fig. 1G) (period of initial cycle of oscillation is 12 ± 4 s) that damped to a steady, elevated base line within 115 ± 48 s (230 measurements on 30 cells, three experiments). (iii) In the third response pattern, cells did not oscillate, but exhibited a step-response, where $Ca^{2+}{}_i$ remained elevated

Section of Molecular Neurobiology, Howard Hughes Medical Institute and Yale University School of Medicine, New Haven, CT 06510.

* Present address: Department of Molecular and Cellular Physiology, Stanford Medical School, Stanford, CA 94305.

indefinitely (Fig. 1H). Even in the absence of applied glutamate, spontaneous Ca^{2+}_i oscillations occurred in a few astrocytes.

The initial increase in Ca^{2+}_i observed in all cells was spatially uniform, however, the Ca^{2+}_i changes underlying both sustained and damped oscillations could be resolved into spatially propagating Ca^{2+}_i waves. Intracellular waves traveled approximately 19 μm/s, eventually involving every portion of the cytoplasm before a subsequent wave began (Fig. 2). Also, decreases in oscillation frequency corresponded to decreases in the underlying intracellular wave velocity.

In confluent astrocytes, waves of Ca^{2+}_i increase propagated from cell to cell (Fig. 3). The spread of Ca^{2+}_i increase is described as a propagating wave because the shape of temporal Ca^{2+}_i change is characteristic and is similar for each point in the path (Fig. 3F). Propagation between cells proceeds with no obvious discontinuity at nearly the same velocity as propagation within cells. Even at the level of individual cells, intercellular waves are distinguished from simple oscillations by the comparatively larger amplitude and the associated plateau phase of the Ca^{2+}_i peaks (Fig. 1H, asterisks). The fraction of intracellular waves that propagated intercellularly varied, although in one fairly typical set of experiments 62 ± 9% of the intracellular waves propagated partially or completely into a neighbor (40 intracellular waves, five experiments). The most extended intercellular wave recorded traveled 772 μm in 51 s and involved 59 cells before moving beyond the field of view.

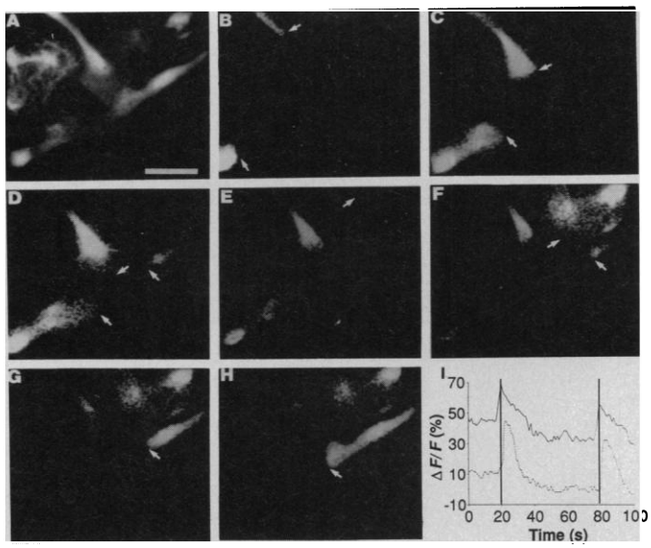

Fig. 2. Waves of Ca^{2+}_i elevation propagating within glutamate-stimulated astrocytes. (**A**) Fluorescence of four fluo-3-loaded cells before glutamate exposure. (**B** through **H**) Fluorescence change images produced by subtracting the digitized base-line image (A) from images digitized at 6-s intervals (6, 12, 18, 24, 30, 36, and 42 s) after the cell had been exposed to glutamate for 40 s. Arrows indicate propagating wave fronts. Intracellular wave velocities range from 9.4 to 61.2 μm/s (mean velocity = 19 ± 9 μm/s; 20 cells from five experiments). (**I**) The phase shift associated with spatial propagation is illustrated with traces made from two different points 67 μm apart in the cell marked by an arrow in (H). *F*, fluorescence. Scale bar, 100 μm.

Astrocytes produced Ca^{2+}_i spikes at glutamate concentrations of 100 n*M* or higher (Fig. 4A) with 50% responding at approximately 300 n*M*. Glutamate concentration also influenced whether oscillations occurred, the frequency of oscillations, and whether both intracellular and intercellular waves were observed. We compared oscillation periods of 20 astrocytes at four glutamate concentrations and found that average oscillation periods decreased with increasing agonist (glutamate concentrations and associated periods were as follows: 0.1 μ*M*, 24.7 s; 1 μ*M*, 16.5 s; 10 μ*M*, 14 s; and 100 μ*M*, 11.3 s), in agreement with studies of similar oscillations in other cell types (*6, 7*). At low concentrations (<1 μ*M*), distinct areas of an astrocyte flickered asynchronously, and intracellular waves typically propagated only through portions of cells. At higher concentrations (1 to 10 μ*M*), Ca^{2+}_i waves more commonly propagated through entire cells, and intracellular waves began to propagate into neighboring cells. At still higher concentrations (10 to 100 μ*M*), intercellular waves began to propagate over long distances. At 1 m*M* glutamate, however, most cells showed a step-rise in Ca^{2+}_i with few oscillations and no intercellular waves.

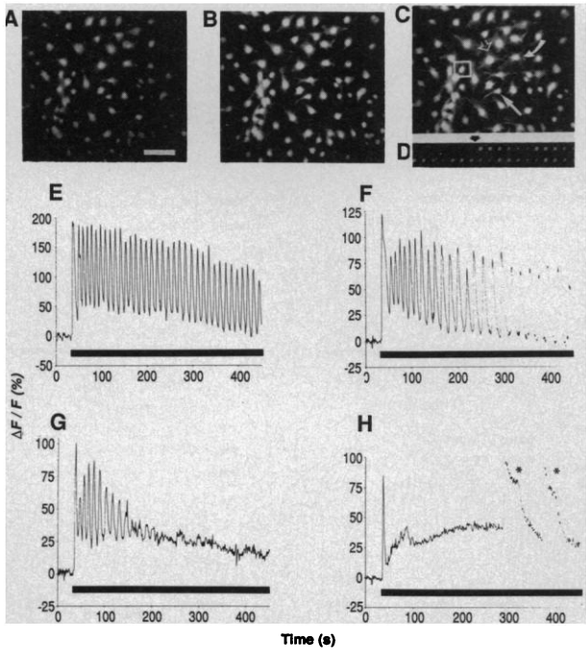

Fig. 1. Glutamate-induced variations in fluorescence (*F*) of cultured hippocampal astrocytes loaded with the Ca^{2+} indicator dye fluo-3. Increased fluorescence intensity indicates increased Ca^{2+}_i. (**A** through **D**) Digital fluorescence micrographs: (A) 6 s before glutamate application, (B) 2 s, and (C) 10 s after glutamate application. (D) A time series of micrographs, sampled at 2-s intervals from the area of the box in (C), showing the initial response to glutamate application (arrowhead) followed by sustained oscillation. (**E** through **H**) Traces showing fluorescence of four individual cells, normalized to base-line values, as a function of time. Glutamate application (100 μ*M*) is indicated by the solid bar between the trace and the horizontal axis. Four different glutamate response patterns are illustrated (E) A sustained-oscillator cell [same cell as (D)], showing the constant frequency form of this response. (F) Another sustained-oscillator cell [solid arrow in (C)], demonstrating the decreasing frequency characteristic. (G) A damped-oscillator cell [curved arrow in (C)]. (H) A step-responder cell [open arrow in (C)]. This cell participates in two intercellular waves appearing in the trace as two peaks, indicated by asterisks. Scale bar, 200 μm.

To determine whether glutamate elicits the initial Ca^{2+}_i spike and subsequent waves by means of the glial Na^+- or Cl^--dependent glutamate uptake systems, we replaced these ions with choline and isethionate. In Na^+-free saline solution, astrocytes showed an initial spike and the same three categories of cellular responses as they did in normal saline (Fig. 4B). Similarly, Cl^--free saline did not block the response of astrocytes to glutamate. It appears that glutamate acts through a receptor distinct from the known astrocytic glutamate uptake systems.

Experiments were carried out in Ca^{2+}-free saline (with EGTA added) to assess the role of surface membrane Ca^{2+} fluxes in the observed responses. Glutamate was still able to elicit Ca^{2+}_i increases and a few cycles of oscillation in Ca^{2+}-free saline (Fig. 4C), indicating that glutamate can liberate Ca^{2+}

from intracellular stores. Neither the lasting base-line elevations nor the sustained oscillations were seen when extracellular Ca^{2+} was absent, implying that surface Ca^{2+} fluxes are required for either sustained Ca^{2+}_i elevation or sustained oscillation.

Specific glutamate receptor agonists confirmed the presence of receptors preferring kainate and quisqualate but not *N*-methyl-D-aspartate (NMDA). Quisqualate (100 μM) mimicked a response to glutamate by inducing an initial Ca^{2+} spike, followed by oscillations, although sustained responses again required the presence of external Ca^{2+} (Fig. 4D). After kainate application (100 μM), every cell showed a single step-rise in Ca^{2+}_i without subsequent oscillations (Fig. 4E). Kainate was without effect in Ca^{2+}-free saline (Fig. 4E), suggesting that glutamate and quisqualate act in part through a receptor that is not activated by kainate. NMDA (100 μM) with glycine (10 μM) had no effect (Fig. 4F). The different responses to quisqualate and kainate in Ca^{2+}-free saline suggest that a quisqualate-preferring receptor mainly releases Ca^{2+} from internal stores, whereas a kainate-preferring receptor mainly activates Ca^{2+} influx through the surface membrane.

We further tested for glutamate receptor subtypes with antagonists. 6-Cyano-7-nitroquinoxaline-2,3-dione (CNQX) had little effect at a concentration (10 μM) that effectively antagonizes a quisqualate receptor–gated ionophore of neurons (*8*). However, at 100 μM, CNQX blocked the initial spike in most cases, depressed damped oscillator responses, and decreased the oscillator frequency and amplitude (Fig. 4G). This receptor resembles a second, relatively CNQX-insensitive metabotropic quisqua-

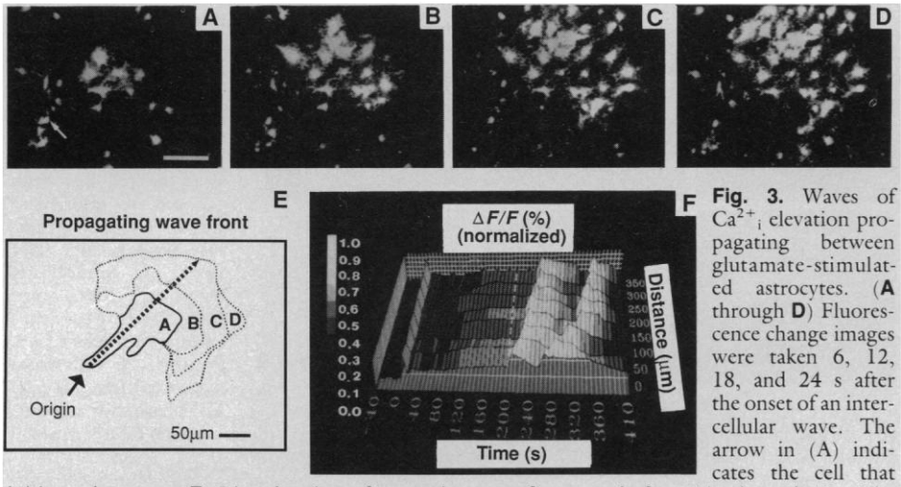

Fig. 3. Waves of Ca^{2+}_i elevation propagating between glutamate-stimulated astrocytes. (**A** through **D**) Fluorescence change images were taken 6, 12, 18, and 24 s after the onset of an intercellular wave. The arrow in (A) indicates the cell that initiates the wave. (**E**) Line drawing of successive wave fronts made from (A) through (D). The dashed line represents a 0-μm trajectory crossing eight different astrocytes. (**F**) Time-course traces from eight positions at 50-μm intervals along the trajectory in (E) were plotted in three dimensions. The distance axis represents the distance from the cell of origin (A) along the trajectory. As Ca^{2+} rises, the gray scale at left, expressed in $\Delta F/F(\%)$ (normalized) moves from black to white. At time zero, after a 40-s base line, glutamate initiates a spike in all eight cells simultaneously. Fluorescence of each cell returns to an elevated base line and then slowly rises with time. At 180 s after the application of glutamate began, the first of two intercellular waves is initiated, indicated by the white peaks. Here, the dashed line indicates the time point when the first cell initiated the wave. A second intercellular wave is initiated in the same cell at 250 s and follows the same path. Intercellular waves propagate with an average velocity of 15 ± 3 μm/s (ten different waves in eight experiments). Scale bar, 200 μm.

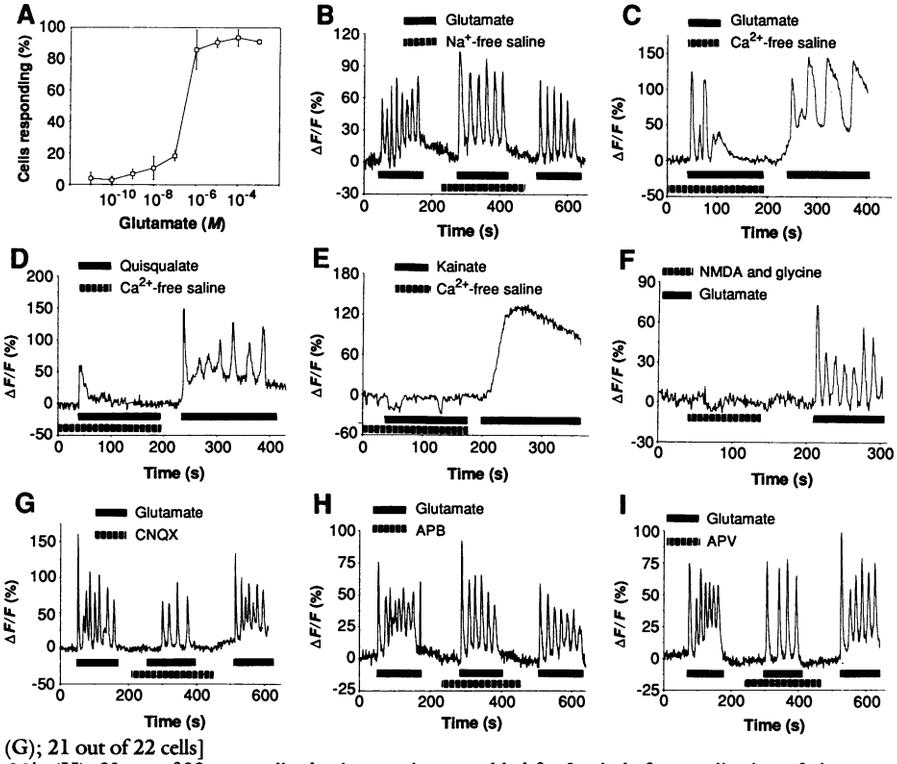

Fig. 4. Pharmacology of glutamate receptor effects on astrocytes. The application of agonist, antagonist, or change of superfused saline is indicated in each graph by a bar or set of bars between the trace and the horizontal axis. (**A**) Glutamate dose-response curve (each point represents data pooled from 80 to 400 cells from three to five experiments). Cells were scored as responding if they showed a Ca^{2+}_i spike on application of glutamate. (**B**) A single cell's fluorescence (F) response to glutamate (100 μM) in Na^+-free saline, preceded and followed by the cell's response to glutamate in normal saline. The amplitude and duration of glutamate-induced Ca^{2+}_i spikes were almost invariably enhanced in Na^+-free saline (16 out of 18 cells). Removal of Na^+ without glutamate application also caused a Ca^{2+}_i rise in many cells. (**C** through **E**) Glutamate (100 μM) (109 out of 146 cells), quisqualate (100 μM) (17 out of 22 cells), and kainate (100 μM) (63 out of 67 cells) effects, respectively, in Ca^{2+}-free saline followed by the same agonists in normal saline. Cells were perfused in Ca^{2+}-free saline for 80 s before the beginning of these recordings. After exposure to agonist in Ca^{2+}-free saline there was a 3-min break in recording (not shown) where the cells were perfused with Ca^{2+}-free saline without agonist. (**F**) NMDA (100 μM) and glycine (10 μM) were unable to elicit a response (73 out of 76 cells). Glutamate (100 μM) was added later to show that the cell was capable of responding. (**G** through **I**) Effects of glutamate receptor antagonists on glutamate (10 μM)-induced Ca^{2+}_i oscillations. CNQX [100 μM in (G); 21 out of 22 cells] reduced both the frequency and amplitude, APB [1 mM in (H); 31 out of 33 cells] had relatively little effect, and APV [1 mM in (I); 19 out of 21 cells] caused a reduction in the frequency of the oscillation with little effect on amplitude. Antagonist was added for 1 min before application of glutamate and was allowed to remain for another minute after glutamate application ceased.

late receptor (*9*). DL-2-Amino-4-phosphonobutyric acid (APB) (1 m*M*) antagonizes the glutamate receptor of the Cl^--dependent glutamate uptake system (*10*) but had no effect on glutamate (10 μ*M*)-induced Ca^{2+} spikes or waves (Fig. 4H). DL-2-Amino-5-phosphono-valeric acid (APV) (1 m*M*), an NMDA-receptor antagonist, partially attenuated the response (Fig. 4I).

Our studies are consistent with reports showing that astrocytes possess glutamate receptor–operated ion channels of the kainate- and quisqualate-preferring subtypes, but not of the NMDA-preferring subtype (*3, 11*). Kainate could raise $Ca^{2+}{}_i$ by depolarization and voltage-gated Ca^{2+} channels (*12*) or by second messenger systems that promote Ca^{2+} entry (*13*). Quisqualate's effects, on the other hand, are reminiscent of a receptor that activates inositol 1,4,5-trisphosphate (IP_3) production and release of $Ca^{2+}{}_i$ from internal stores (*9*). In fact, quisqualate stimulates inositol turnover in astrocytes (*14*), and the average oscillation frequencies reported here are consistent with systems where $Ca^{2+}{}_i$ oscillations are attributed to IP_3 turnover (*15*).

The $Ca^{2+}{}_i$ waves may propagate between cells by passage of a second messenger through gap junctions (*16*). Gap junctions are a prominent feature of astrocytes in brain (*17*) and have also been observed in our cultures by means of electron microscopy (*18*) and by dye photobleaching experiments (*19*). Potential mediators of the signaling postulated here include IP_3, some other PI metabolite, the Ca^{2+} ion itself, and the flow of electric current (*15, 20*). Although electric current flow may somehow act as a junctional coupling factor, the slow propagation of intercellular $Ca^{2+}{}_i$ waves probably rules out any simple cable propagation mechanisms.

We have seen a variety of oscillatory and nonoscillatory $Ca^{2+}{}_i$ responses of cultured astrocytes to the neurotransmitter glutamate. Because glutamate-releasing nerve terminals are close to astrocytic membranes, neuronally released glutamate may trigger $Ca^{2+}{}_i$ responses in astrocytes in situ similar to those we have observed in cell culture (*21*). Also, the apparent encoding of glutamate dose into various forms of oscillation and spatial propagation suggests a system adapted to the long-range transmission of information.

Note added in proof: It has come to our attention that glutamate-induced $Ca^{2+}{}_i$ oscillations have now been observed in cultured astrocytes by using fura-2, a fluorescence-ratio $Ca^{2+}{}_i$ indicator (*22*).

REFERENCES AND NOTES

1. P. Rakic, *Science* **241**, 170 (1988); H. F. Cserr and M. Bundgaard, *Ann. N.Y. Acad. Sci.* **481**, 1 (1986); R. P. Shank and M. H. Aprison, in *Glutamine and Glutamate in Mammals II, Glutamate as a Neurotransmitter*, E. Kvamme, Ed. (CRC Press, Boca Raton, FL, 1988), p. 3.
2. H. Marrero, M. L. Astion, J. A. Coles, R. K. Orkland, *Nature* **339**, 378 (1989); B. A. Barres, L. L. Y. Chun, D. P. Corey, *Neuron* **2**, 1375 (1989); *Glia* **1**, 10 (1988).
3. M. M. Usowicz, V. Gallo, S. G. Cull-Candy, *Nature* **339**, 380 (1989).
4. Mixed hippocampal cultures [S. Finkbeiner and C. F. Stevens, *Proc. Natl. Acad. Sci. U.S.A.* **85**, 4071 (1988)] were plated at low density (1000 cells/cm^2) on glass cover slips coated with collagen and poly-D-lysine. Cultures matured 1 to 3 weeks before they were used for experiments. These cultures stained positively (>98% of cells) with antibodies to glial fibrillary acidic protein and negatively (>98% of cells) with antibodies to A2B5, indicating these were type-I astrocytes according to a classification of optic nerve astrocytes [M. C. Raff, E. R. Abney, J. Cohen, R. Lindsay, M. Noble, *J. Neurosci.* **3**, 1289 (1983)]. Cultures were loaded with fluo-3 in the acetomethoxyester form (fluo-3AM) (5 μ*M*) for 1 hour and were mounted in a flow-through perfusion chamber [P. Forscher, L. K. Kaczmarek, J. Buchanan, S. J. Smith, *ibid.* **7**, 3600 (1987)]. Cells were superfused at room temperature with normal saline (137 m*M* NaCl, 5.3 m*M* KCl, 3 m*M* $CaCl_2$, 1 m*M* $MgCl_2$, 10 m*M* Hepes, and 25 m*M* glucose) during base line and drug washout periods. Superfused drugs equilibrated with cells within 5 s of application. Images were collected on an inverted microscope (Zeiss IM-35) with mercury arc illumination, a wide-band fluorescein isothiocyanate filter set, a ×25, 0.8 numerical aperture objective (Zeiss Plan Neofluar), a silicon-intensifier target tube (SIT) camera (Hamamatsu C-2400), a digital image processor (Imaging Technology series 151), and an optical memory disk video recorder (Panasonic TQ-2026F). Each image is an average of eight successive video frames. A computer-controlled shutter was used to eliminate unnecessary specimen illumination. Images and calibration data were recovered from optical disk for quantitative analysis with a frame grabber (Imaging Technology PFGplus-640). All data were corrected for video system offset errors with an optical calibration procedure. Time-course traces were generated by averaging over an area of 5 by 5 pixels.
5. We chose fluo-3 as the Ca^{2+} indicator for this study because, among all presently available indicators, it provides the largest optical signal per molecule and thus allows for detection of Ca^{2+} transients in the smallest possible cytoplasmic volumes [J. P. Kao, A. T. Harootunian, R. Y. Tsien, *J. Biol. Chem.* **264**, 8179 (1989)]. In this study, we detected Ca^{2+} signals in regions where the astrocyte cytoplasm was barely 1 μm thick. One drawback of this indicator, however, lies in its lack of a spectral shift on binding Ca^{2+}. This means that fluo-3 cannot provide direct information about steady-state Ca^{2+} levels and cannot produce the calibrated ratio images familiar from work with the excitation-shift Ca^{2+} indicator fura-2. Nonetheless, fluo-3 signals can be normalized for path length and dye concentration variations against base-line fluorescence (F_0), and the resulting data ($\Delta F/F_0$ or simply $\Delta F/F$) can provide useful and extremely sensitive information about transient Ca^{2+} deviations from base-line levels. Fluo-3 was thus suitable for the present study where the data of interest (spikes, oscillations, and waves) were transient in nature.
6. N. M. Woods *et al.*, *Nature* **319**, 600 (1986).
7. R. Jacob *et al.*, *ibid.* **335**, 40 (1988).
8. T. Honoré *et al.*, *Science* **241**, 701 (1988); K. Yamada, J. M. Dubinsky, S. M. Rothman, *J. Neurosci.* **9**, 3230 (1989).
9. H. Sugiyama, I. Ito, M. Watanabe, *Neuron* **3**, 129 (1989); H. Sugiyama, I. Ito, C. Hirono, *Nature* **325**, 531 (1987); F. Sladeczek, M. Recasens, J. Bockaert, *Trends Neurosci.* **11**, 545 (1988).
10. J.-P. Pin, J. Bockaert, M. Recasens, *FEBS Lett.* **175**, 31 (1984); D. D. Schoepp and B. G. Johnson, *J. Neurochem.* **50**, 1605 (1988).
11. C. L. Bowman and H. K. Kimelberg, *Nature* **311**, 656 (1984); H. Kettenmann and M. Schachner, *J. Neurosci.* **5**, 3295 (1985).
12. B. A. MacVicar, *Science* **226**, 1345 (1984); B. A. Barres, L. L. Y. Chun, D. P. Corey, *J. Neurosci.* **9**, 3169 (1989).
13. R. Penner, G. Matthews, E. Neher, *Nature* **334**, 499 (1988); J. Vilven and R. Coronado, *ibid.* **336**, 587 (1988).
14. B. Pearce, J. Albrecht, C. Morrow, S. Murphy, *Neurosci. Lett.* **72**, 335 (1986).
15. M. J. Berridge and R. F. Irvine, *Nature* **341**, 197 (1989); T. J. Rink and R. Jacob, *Trends Neurosci.* **12**, 43 (1989). Others [B. A. MacVicar, S. A. Crichton, D. M. Burnard, F. W. Y. Tse, *Nature* **329**, 242 (1987)] have observed membrane voltage and input resistance oscillations in astrocytes from kainate-lesioned hippocampal slices in response to application of the phorbol ester, 12-*O*-tetradecanoyl phorbol-13-acetate. On average, these voltage oscillations are about an order of magnitude higher in frequency than the $Ca^{2+}{}_i$ oscillations we observed. MacVicar *et al.* raise the possibility that $Ca^{2+}{}_i$ oscillations, mediated by protein kinase C downregulation, might underlie these voltage oscillations.
16. J. C. Saez *et al.*, *Proc. Natl. Acad. Sci. U.S.A.* **86**, 2708 (1989); P. Brehm, J. Lechleiter, S. J. Smith, K. Dunlap, *Neuron* **3**, 191 (1989).
17. A. Peters, *J. Anat.* **96**, 237 (1962).
18. J. Buchanan and C. F. Stevens, unpublished observations.
19. S. M. Finkbeiner, unpublished observations.
20. P. Graf, S. VomDahl, and H. Sies [*Biochem. J.* **241**, 933 (1987)] have extended observations made on single hepatocytes (*6*) by demonstrating that an entire organ, the liver, can show synchronous agonist-induced Ca^{2+} oscillations. Hepatocytes, like astrocytes, are extensively coupled by gap junctions.
21. How might synaptic glutamate release in the brain relate to global superfusion in culture? The astrocyte Ca^{2+} responses described in this report were induced by glutamate superfusion, a spatially uniform stimulus. Nonetheless, propagating Ca^{2+} waves were observed. Astrocytes in situ would probably experience more localized sources of glutamate, for example, in the vicinity of specific synapses. Under these circumstances, the Ca^{2+} wave mechanism might convey information about localized synaptic glutamate release to remote sites over the extent of a single astrocyte's processes or over the extent of coupled networks of astrocytes.
22. A. M. Jensen and S. Y. Chiw, *J. Neurosci.*, in press.

23. We thank B. Friedman for the antibodies to A2B5. Supported by NIH grants NS16671-09 to S.JS., NS 12961-14 to C. F. Stevens, and GM 07205 to S.M.F. and by Howard Hughes Medical Institute funding to S.JS. and C. F. Stevens).

22 August 1989; accepted 27 October 1989